

## Karst Identification from Core and Thin Section in Jintan Platform, Central Luconia Province, Malaysia

Bing Bing Saw<sup>1,4\*</sup>, Siti Sarah Ab Rahman<sup>1,5</sup>, Grisel Jimenez Soto<sup>2</sup>, Choong Chee Meng<sup>3,5</sup>, Nurul Huda M Jamin<sup>3</sup>

<sup>1</sup> South East Asia Clastic/Carbonate Research Laboratory, Institute of Hydrocarbon Recovery, Universiti Teknologi PETRONAS, Seri Iskandar, Perak 32610, Malaysia

<sup>2</sup> Centre for Subsurface Imaging, Institute of Hydrocarbon Recovery, Universiti Teknologi PETRONAS, Seri Iskandar 32610, Malaysia

<sup>3</sup> Department of Geoscience, Universiti Teknologi PETRONAS, Seri Iskandar, Perak 32610, Malaysia

<sup>4</sup> PETRONAS Carigali Sdn. Bhd., PETRONAS Twin Tower 2, 50470, Kuala Lumpur, Malaysia

<sup>5</sup> Digital Geoscience Global Sdn. Bhd., Binjai 8, Lorong Binjai, 50400, Kuala Lumpur, Malaysia

Received March 18, 2022, Accepted December 1, 2022

---

### Abstract

The Miocene carbonate platforms of Central Luconia are an important gas prolific in offshore Malaysia. Extensive studies have been done in the past 40 years but the formation of karst in Central Luconia still largely remained understudied. This paper aims to study the microfacies of karst intervals on the Jintan Platform and integrate the relationship between the sedimentology, petrophysics and the paleo-sea level fluctuations during the Miocene. The information from core data of several karst intervals is mainly white to beige limestone, preserved as rubble pieces or “chalky” appearance. Three lithofacies and five microfacies are evident in the karst zones. The observed lithofacies are (1) foraminiferal and skeletal debris wackestone-packstone, (2) coral float-stone-rudstone, and (3) algal and skeletal wackestone-packstone; and microfacies are (1) foraminiferal-skeletal packstone/floatstone, (2) coral-skeletal floatstone, (3) skeletal wackestone/floatstone, (4) coral framestone, and (5) foraminiferal-algal packstone/rudstone. The sea-level lowstand during the Miocene caused the carbonate platforms exposed to the surface leading to the karstic formation by active diagenetic processes. Dissolutions create mouldic pores and vugs which can be observed in the cores and thin sections. Tectonic evolution could have impacted besides eustasy sea-level control, but it does not present the karstification that occurred along the fault plane, as previous workers showed. Therefore, the control of karstification remains controversial whether it is due to a tectonic modification or sea-level lowstand resulting in meteoric diagenesis alone.

**Keywords:** Miocene; Paleo sea-level; Vugs; Mouldic; Wireline logs.

---

## 1. Introduction

Carbonate karst is one of the research highlights in the carbonate reservoir geology that attracts the attention of scientists worldwide. Carbonate karst is a diagenetic facies, an overprint in subaerially exposed carbonate bodies, produced and controlled by dissolution and migration of calcium carbonate in meteoric waters, occurring in a wide variety of climate and tectonic settings, and generating a recognizable landscape [1]. The dissolution process creates substantial pores, vugs, and caves. Greater cave volume is developed in fine-grained micritic rocks than in coarser-grained rocks since the smaller grain size gives a greater amount of surface available for percolating waters [2]. Karst presents a generalized facies pattern that can be summarized into 3 phases: (1) Infiltration (upper vadose zone) consists of white, fine-grained chalky deposits or collapse breccia, abundantly colonized by fungi and bacteria; (2) Percolation (lower vadose zone) shows little dissolution, but the lower part near the phreatic

water table is favourable for speleothem formation; (3) Lenticular (phreatic zone) characterized by the intense formation of subhorizontal caves. Most of the cavern porosity is produced in this zone, especially just below the water table [1,3].

Karst-related reservoirs commonly show great heterogeneity [4-5], which complicates exploration for oil and gas [6]. Dissolution leads rocks to collapse and karst breccias to form [6], given difficulty in well planning (problem with mud losses and completion length), well management and development strategy, and hydrocarbon volume calculation [7]. The karst in Central Luconia has been studied for decades but the formation of karst remains poorly understood. By using the comprehensive data from drilling, cores and thin section of the Jintan Platform, this paper aims to: (1) study the microfacies of karst intervals, (2) integrate the relationship between the sedimentology, petrophysics and the paleo-sea level.

## 2. Geological setting and study area

The Central Luconia Province is situated in the South China Sea, approximately 100-300 km offshore Sarawak, NW Borneo. It is of some 45,000 km<sup>2</sup>, and over 250 carbonate buildups contain hydrocarbons, with some 65 tcf of recoverable gas and some minor oil reserves reported [8-11]. Episodes of rifting of the South China Basin during Oligocene to middle Miocene resulted in the formation of the SW-NE trending horst-graben system [12]. These elevated blocks played a significant role in the topography that initiated the growth of numerous carbonate buildups. The carbonate deposition started during the middle Miocene (Cycle IV) to late Miocene (Cycle V), and terminated between the end of late Miocene to Pleistocene (Cycle VI-VIII), most likely due to the influx of siliciclastics from the SW and SE of Borneo Island.

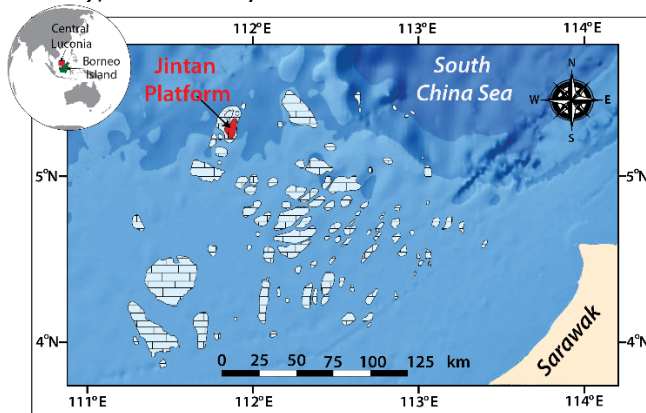


Figure 1. Location map of Jintan Platform, offshore Malaysia

This study will focus on the Jintan Platform (Figure 1), which is located in the NW part of Central Luconia, farther away from the siliciclastic wedge. It originated on one of the structural highs formed by regional extension and faulting during the Palaeocene to early Miocene [13]. The Jintan Platform is 30 km x 50 km wide, and about 1200 m thick. Stratigraphically, it belongs to the Cycle IV-V carbonate sequence (middle to late Miocene) (Figure 2). The carbonate sequence consists entirely of limestone with minor argillaceous limestone, mainly deposited within a reefal buildup

facies in a relatively shallow, inner neritic marine environment [13].

## 3. Methodology

Core description, thin section analysis, well logs interpretation, quantification of macro-porosity (mouldic and vugs), and Strontium (Sr) isotope data are used to determine the properties of karst intervals and the architecture of Mega Platform.

### 3.1. Core description

Two cores of the wells Jintan-2 and Jintan-3 were described (Figure 3). Cores were cut at carbonate intervals, 1613-1697 m in Jintan-2, and 1654-1854.5 m in Jintan-3. The core description included lithology, grain size, Dunham texture, components and visual pores that helped to identify lithofacies within the carbonate succession.

### 3.2. Petrographic analysis

Thirty-three thin sections from the karst interval zones were selected for petrographic analysis. They were stained with Alizarin Red-S to differentiate calcite or dolomite. The petrographic analysis was carried out using Olympus digital BX-43 microscope with a DP 72 digital

camera. The recognized microfacies and porosity types were described according to the schemes proposed by Dunham [14] and Embry and Klovan [15]; and Choquette and Pray [16], respectively. The Sr-isotope data is from the CSIRO report [17] to integrate and correlate with the growth history of the Jintan Platform.

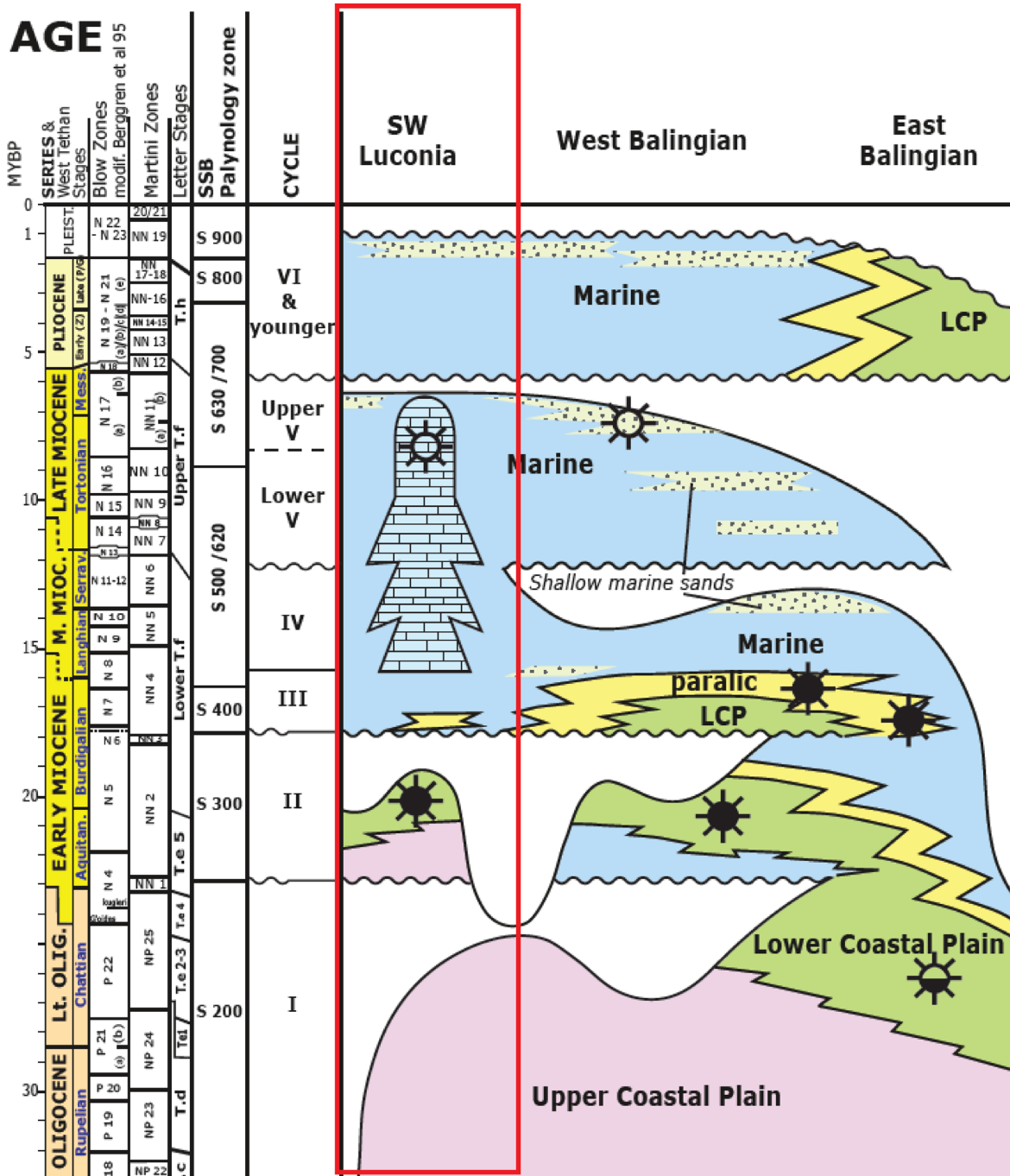


Figure 2. An updated diagram for the cycles and stratigraphic column of Central Luconia (red box) (re-drawn from Veenhof, [36], with a modern time scale; similar diagrams to this are also found in Shell reports from the late 1980's; adapted from Lunt, [37]).

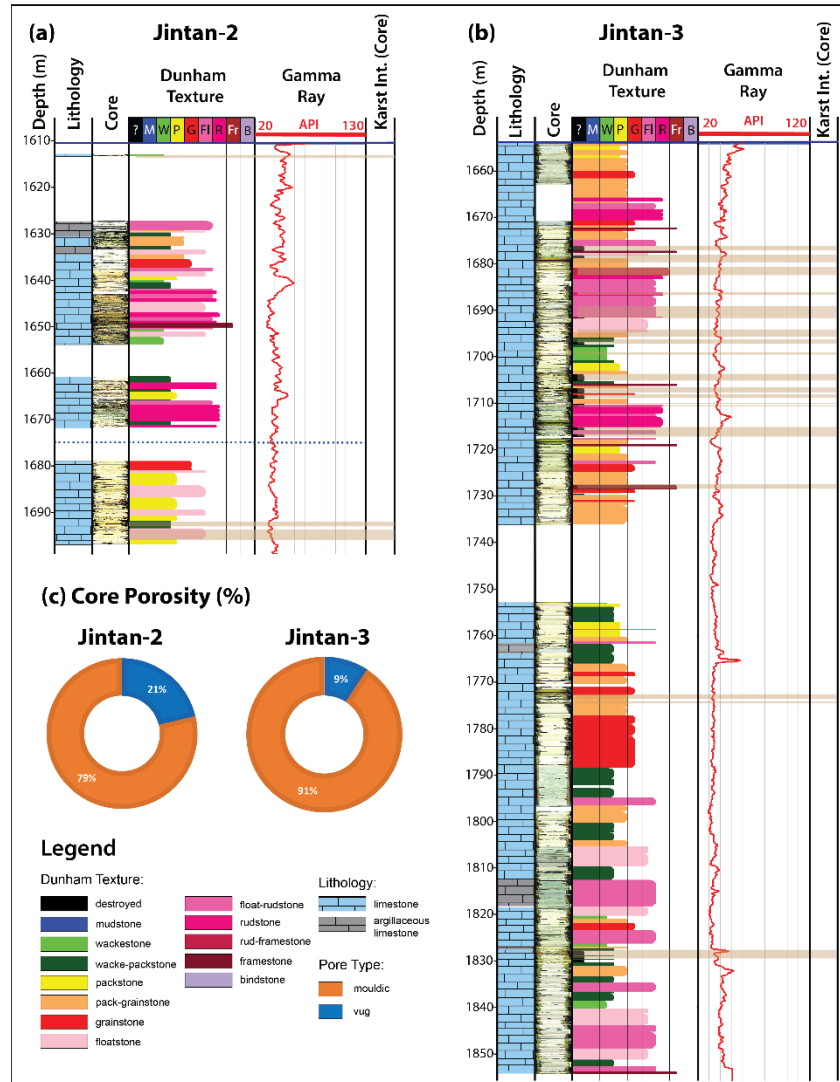


Figure 3. Core description of (a) Jintan-2 and (b) Jintan-3 on a scale of 1:1000. (c) Quantitative distribution of core porosity at the karst zones. Mouldic porosity is commonly observed in the dissolved skeletal components, probably foraminifera, echinoids or bivalves. Vuggy porosity was observed in the massive or branching corals.

### 3.3. Petrophysical analysis

The karst features were identified from 2 conventional logging characteristics, in particular, gamma-ray (GR), resistivity (LLD), neutron-porosity (PORNET) and permeability (PERMNET) logs. Drilling reports, mud logging data, and a summary of daily and final well reports were reviewed to track the mud loss events in the Jintan Platform. Quantification of porosity (mouldic and vugs) from cores and thin sections were integrated with PORNET and PERMNET and other conventional wireline logs.

## 4. Results and discussions

### 4.1. Description of karst intervals

The karst zones of the cores of wells Jintan-2 and Jintan-3 were described (Figure 3). The limestone is white to beige, preserved as rubble pieces, loosed, demonstrating the “chalky” appearance (Figure 4). The dissolution characteristics of pores can be directly observed from the cores at the lower part of Jintan-2 and the upper part of Jintan-3. No pore-cave was

observed in both wells as the cores cannot be cut through the large karst or cave. Two major porosity types, mouldic and vugs were recognized in both wells (Figure 3, Figure 4). The mouldic pore size ranges from 1 mm to 2 mm, commonly observed in the dissolved skeletal components, probably foraminifera, bivalves or echinoids. The vug pore size ranges from 4 mm to 23 mm, spotted in the branching and massive corals. The fractured porosity is rare and only noticed within the massive corals.

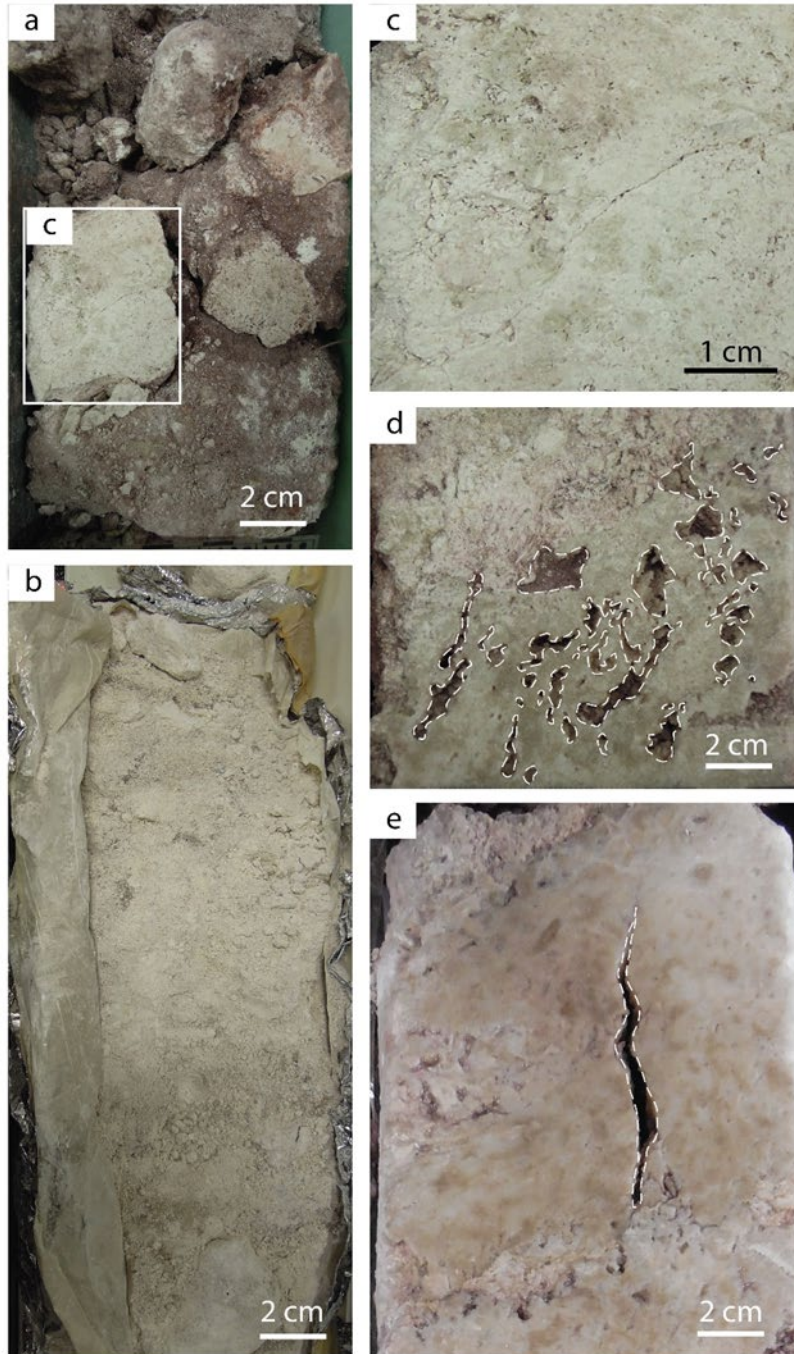


Figure 4. The observed rock type and the common pore types occur in the karst zones. (a) Rubble pieces. (b) Chalkified limestone. (c) Mouldic pores. (d) Dissolution vugs. (5) Fracture observed within the massive coral

## 4.2. Lithofacies types

Three major limestone lithofacies were identified based on preserved rubble pieces. These lithofacies are (1) foraminiferal and skeletal debris wackestone-packstone, (2) coral floatstone-rudstone and (3) algal and skeletal wackestone-packstone.

### 4.2.1. Foraminiferal and skeletal debris wackestone-packstone

The foraminiferal and skeletal debris wackestone-packstone lithofacies is predominantly limestone, containing mainly larger benthic foraminifera and skeletal debris including the fragmented bivalves, gastropods, echinoids and coral debris. This facies is possibly deposited in a low energy water condition, possibly in a protected back-reef shallow lagoonal setting.

### 4.2.2. Coral floatstone-rudstone

The coarser debris of coral floatstone-rudstone lithofacies is limestone, consisting mainly of Scleractinian branching corals and massive corals debris associated with larger benthic foraminifera, red algae, bivalves and echinoids. The fragmented coral debris could be either transported from the reef crest to the proximal lagoonal environment or collapsed within the reef crest environment or bedrock/celling of an underlying cavity or cave.

### 4.2.3 Algal and skeletal wackestone-packstone

The algal and skeletal wackestone-packstone is limestone. It commonly consists of red algae associated with larger benthic foraminifera, coral debris and skeletal debris. This facies is deposited in a low water energy condition, suggesting a protected back-reef shallow lagoon environment.

## 4.3. Microfacies types

The lithofacies were integrated with petrographic analysis data. Five microfacies were distinguished from the karst interval of the Jintan Platform. They are (1) foraminiferal-skeletal packstone/floatstone, (2) coral-skeletal floatstone, (3) skeletal wackestone/floatstone, (4) coral framestone, and (5) foraminiferal-algal packstone/rudstone. These microfacies are shown in Figure 5. The microfacies corresponding to lithofacies types is presented in Table 1.

### 4.3.1. Foraminiferal-skeletal packstone/floatstone

The foraminiferal-skeletal packstone/floatstone consists of moderately to poorly sorted allochems. It is mainly composed of larger benthic foraminifera and red algae associated with echinoids, bivalves, bryozoa, coral fragments, and planktonic foraminifera. The foraminifera are *Cycloclypeus*, *Operculina* and *Lepidocyclina*. The occurrence of diverse fauna suggests an open marine environment. The occurrence of *Cycloclypeus* and rare planktonic foraminifera indicates a fore-reef depositional environment [18-20]. It could relate to the rapid flooding caused by the rising sea level.

### 4.3.2. Coral-skeletal floatstone

The coral-skeletal floatstone commonly consists of coral debris, with less common in larger benthic foraminifera, bivalves and echinoids, and rare in red algae and gastropods. The larger benthic foraminifera are *Operculina* and miliolids. The fragmented coral debris could be transported to a proximal lagoonal environment. The existence of miliolids and *Operculina* indicate a protected area and a reef or near reef environment [18,21-23].

### 4.3.3. Skeletal wackestone/floatstone

The skeletal wackestone/floatstone is the most common microfacies distinguished in the karst intervals. This microfacies commonly consists of larger benthic foraminifera, bivalves and echinoids, with less common in red algae, gastropods, coral fragments and brachiopods. The larger foraminifera are *Operculina*, *Sorites*, *Marginopora*, *Sphaerogypsina*, and miliolids. This microfacies has a higher micritic content. The miliolids, *Operculina*, *Sorites*, and *Marginopora* indicate an open shallow marine, protected back-reef environment [18,21-23,35].

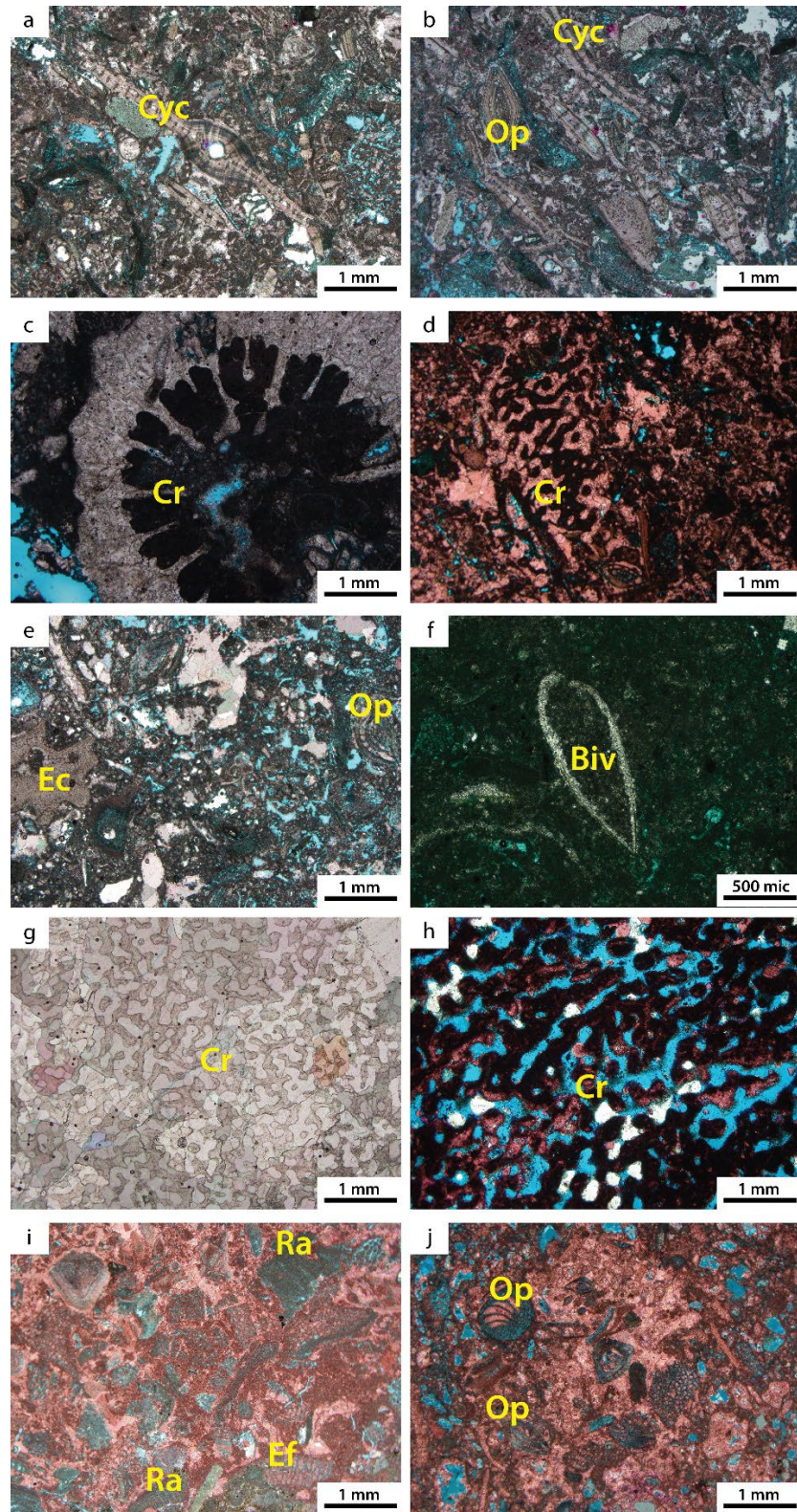


Figure 5. Microfacies of Jintan Platform. All these photomicrographs are taken under plane polarised light (PPL). (a, b) Foraminiferal-skeletal packstone/floatstone. (c, d) Coral-skeletal floatstone. (e, f) Skeletal wackstone/floatstone. (g, h) Coral framestone. (i, j) Foraminiferal-algal packstone/rudstone. Abbreviation: larger benthic foraminifera – Cyc: *Cycloclypeus*, Op: *Operculina*, Ef: Encrusting foram; Cr: coral; Ec: echinoid; Biv: bivalve; Ra: red algae

#### 4.3.4. Coral framestone

This microfacies is the least common to be observed in the karst intervals compared to the other microfacies. The coral framestone is composed of massive corals. Corals grow the best in clean-warm, shallow (within the photic zone) water under high energy conditions, generally in water depths from 1-18 m [24]. However, this microfacies is interpreted to be coral debris shed into the shallowest lagoon environment either from the nearest in-situ colonies that are deposited in a reefal setting or a small patch reef in a lagoonal environment.

#### 4.3.5. Foraminiferal-algal packstone/rudstone

The foraminiferal-algal packstone/rudstone is commonly composed of larger benthic foraminifera (*Operculina*, *Sorites*, *Lepidocyclina*, *Marginopora* and miliolids) and red algae, with less common in bivalves, echinoids, brachiopods, and coral fragments. The common occurrence of *Operculina* is a good indicator of a warm shallow lagoonal environment [25]. This microfacies is deposited in a protected, shallow lagoon environment.

Table 1. Microfacies corresponding to which lithofacies type

Lithofacies type	Corresponding microfacies type
Foraminiferal and skeletal debris wackestone-packstone	Foraminiferal-skeletal packstone/floatstone
	Skeletal wackestone/floatstone
	Foraminiferal-algal packstone/rudstone
Coral floatstone-rudstone	Coral-skeletal floatstone
	Skeletal wackestone/floatstone
	Coral framestone
Algal and skeletal wackestone-packstone	Skeletal wackestone/floatstone
	Foraminiferal-algal packstone/rudstone

#### 4.4. Porosity and cement types

Subaerially exposed leads to dissolution and exhibits meteoric cementation. Large vugs and mouldic pores are a result of the intense dissolution (Figure 6).

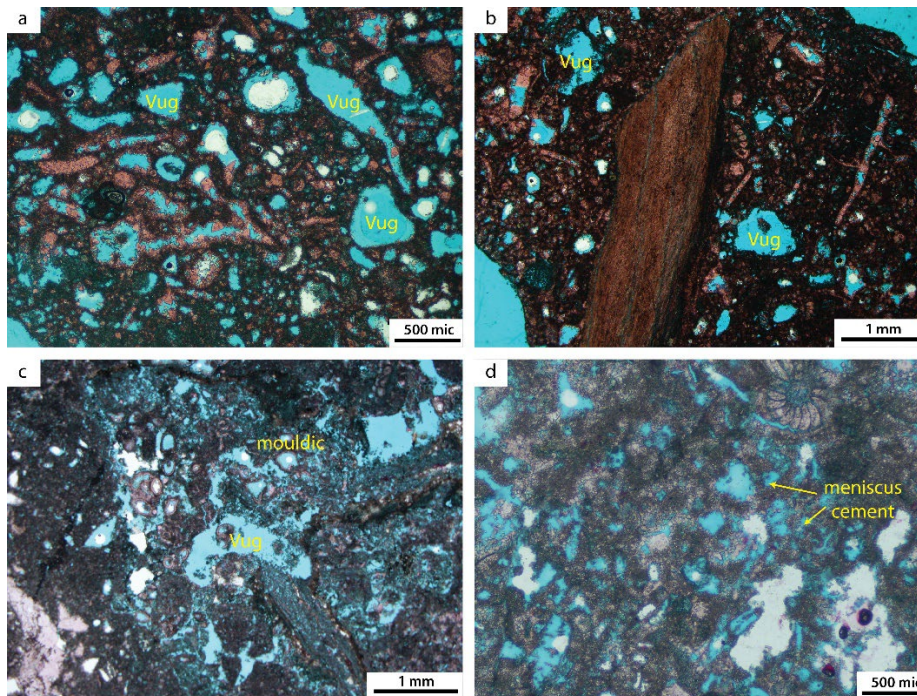


Figure 6. Type of porosity and cement observed in Jintan Platform. (a, b) Vuggy porosity. (c) Mouldic and vuggy porosity. (d) Meniscus cement

Dissolution enhances the porosity but destroys most of the bioclasts partially or completely. Some of the voids are filled with calcite cement. Meniscus calcite cement is evident in the karst zone. Meniscus calcite cement precipitated at or near grain-to-grain contact in pores forming a crescent-shaped body (Figure 6). The size of the crystal is from silt to fine-grained size ( $> 10 \mu\text{m}$  to  $< 100 \mu\text{m}$ ). This cement characteristically formed in the meteoric-vadose zone [26].

#### 4.5. Petrophysical characteristics of karst intervals

The karst features were observed through dissolution mouldic pores, vugs, fractures, chalkified layers and rubble pieces throughout the cores. These karst features were integrated with the petrophysical properties (Figure 7) including Gamma-ray, Caliper, deep resistivity, porosity logs and permeability logs. The logs characteristics are 30.42-57.73 API (GR), 11.74-16.91 inches (Caliper), 0.68-338.05 ohm (LLD), 0.05-0.39 (PORNET) and 0.08-130.29 mD (PERMNET). Minor mud losses were reported in the carbonate section [27] and one of the wells terminated drilling operations due to lost circulation [28].

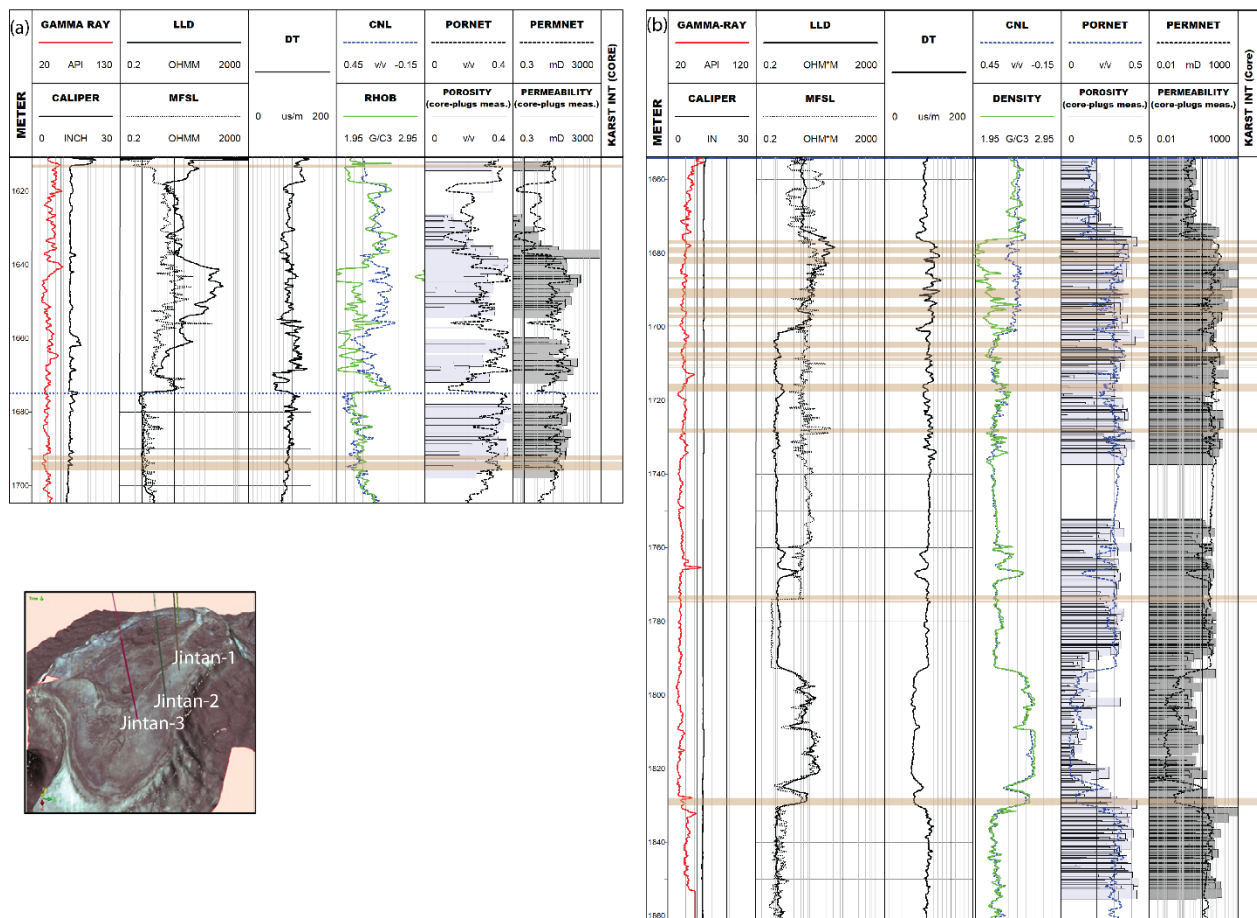


Figure 7. Petrophysical properties of karst intervals. (a) Jintan-2, (b) Jintan-3

#### 4.6. Karst and sea-level fluctuation

Jintan Platform experienced several episodes of subaerial exposure and karstification [13]. Five sequences were analyzed by Yusliandi [29] (Figure 8). The karst zones occurred mostly at Sequence 2 to Sequence 4.

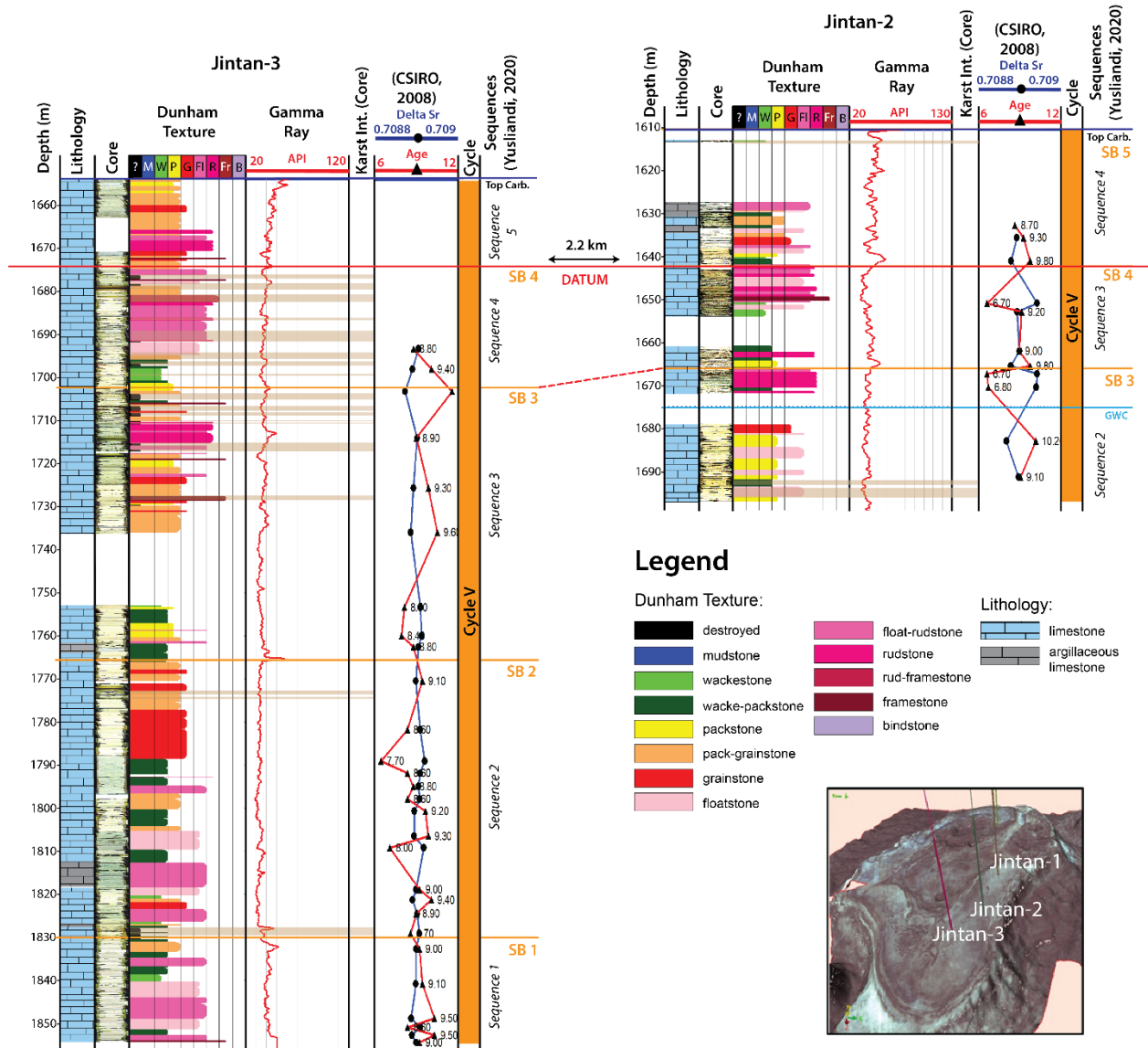


Figure 8. The interpreted sequences of two wells across Jintan Platform

Sequence 2 presents at the lower part of Jintan-2 and Jintan-3. The karst zones generally show high porosity and high permeability in both wells, ranging from 27.4-35.0% in porosity and 20.01-58.88 mD in permeability. Based on the core data, the lithofacies of karst zones represent by foraminiferal/skeletal wackestone-packstone, coral floatstone-rudstone and algal/skeletal wackestone-packstone facies.

The karst intervals of Sequence 3 were only observed at Jintan-3 well. The karst zones show a high porosity and permeability ranging from 23.6-36.6 % in porosity and 25.61-103.14 mD in permeability. It predominantly consists of coral floatstone-rudstone lithofacies.

Carbonates are sensitive to relative sea-level changes. The subaerial exposure and karstification appear more related to sea-level fall than the rapid rise of sea level [13] when the carbonate is totally exposed to meteoric conditions, in which they are more prone to dissolution than mechanical erosion. Therefore, large vugs and mouldic porosity are commonly observed in the Jintan Platform.

The Strontium isotope showed in Figure 8 given the age of the limestone ranging from 6.7 Ma to 10.2 Ma. It is slightly younger compared to the reported microfossil assemblages. The stratigraphic age of the limestone deposits is interpreted as middle Miocene to late Miocene

(lower Tf to upper Tf), Cycle IV-V based on the occurrence of larger benthic foraminifers, *Borelis melo*, *Fosculinella bantangensis* (middle Miocene); *Lepidocyclina spp.* (late Miocene); and planktonic fossils, *Discoaster quinqueramus* (corresponding with NN11 Martini Zone [30], Tortonian to Messinian, late Miocene) [28]. No carbon and oxygen isotope data are available.

Luconia main carbonate platforms generally fall within a period of sea-level highstand during the middle Miocene on the global sea-level curve of Haq [13,32]. As presumed the age of the carbonate in the two wells is Serravallian to Messinian, unfortunately, the exposure events are not exactly pointing to the global sea-level fall. The Jintan Platform tends to be more influenced by the local sea-level fluctuation. Additionally, the subaerial exposure and karstification may lead to the missing or condensed section.

As the sea level fell, the carbonate platforms exposed to the surface postulated that subaerial exposure had terminated the reefs (Cycle V) [13], leading to the karstic formation by active diagenetic processes, despite the transgressive model proposed by Epting [12]. Later Lunt [33] research had mentioned the Cycle V carbonate reefs and microfossils showing drowning sequences rather than karstification, and therefore unlikely to be reef extinctions due to eustatic sea-level fall.

Apart of consider eustasy as a primary controlling force on karstification, tectonic might be one of the main driven origins. Even though Central Luconia was not affected by compressional tectonics as happened in the southern part of the Sarawak shelf during the middle Miocene, but experienced major structuring on the fault-blocking [18]. The karstification of the carbonate platform can occur along a plane of weaknesses due to syn-depositional faulting and fracturing [34]. However, 3D seismic may or may not display similar characteristics of karstification as observed on onshore carbonate buildups (e.g. Subis Limestone) due to timing when the process had taken place and may have been deformed by the overlying siliciclastic units [34]. Therefore, the control of karstification still remains controversial whether is due to a tectonic modification or sea-level lowstand resulting from meteoric diagenesis alone. In this work, we open the discussion about the potential factors that could have been the origin of the karstification network development.

## 5. Conclusions

The karst zones of the Jintan Platform are white to beige limestone, preserved as rubble pieces or chalk appearance. The limestone is predominantly composed of coral fragments, larger benthic foraminifera, echinoids, and bivalves; rare in red algae and gastropods. It is subdivided into three lithofacies and five microfacies.

The exposure events and karstification may have impacted the reservoir quality resulting in most of the limestone within the intervals being high in porosity and permeability. Dissolution vugs, and mouldic porosity are commonly observed in cores and thin sections.

The formation of karstification on the studied Jintan Platform remains an unresolved question whether is due to meteoric diagenesis during sea-level lowstand or tectonic modification.

## Acknowledgements

This research was funded by YUTP-FRG Grant with the cost centre 015LC0-314. The dataset presented in this paper belongs to Malaysia Petroleum Management (MPM). The findings of this paper are contributed to part of Siti Sarah Abdul Rahman's PhD project. The authors are thankful to Universiti Teknologi PETRONAS (UTP), Institute of Hydrocarbon Recovery (IHR), Geoscience Department and The South East Asia Clastic & Carbonate Research Laboratory (SEACARL) for providing the facilities to support this research work. Our thanks are also extended to PETRONAS MPM for permission to use proprietary data for this research. We express our deep gratitude to ALT for providing WellCAD software to conduct this research. This research work is funded by the YUTP grant and SHELL endowment to Universiti Teknologi PETRONAS.

**Conflicts of interest:** The authors declare no conflict of interest.

## References

- [1] Esteban M, and Klappa CF. Subaerial Exposure Environment; Scholle, PA, Debour, DG, and Moore, CH., Eds.; Carbonate Depositional Environment, Oklahoma: AAPG Memoir 33 1983; 2-54.
- [2] Sweeting MM. Karst morphology and limestone petrology. *Progress Physical Geography*, 1979; 3(1): 102-110.
- [3] Thrailkill J. Chemical and hydrologic factors in the excavation of limestone caves. *Geol. Soc. America Bull.*, 1968; 79: 19-46.
- [4] Hopkins JC. Characterization of reservoir lithologies within subunconformity pools: Pekisko Formation, Medicine River field, Alberta, Canada. *AAPG Bulletin*, 1999; 83: 1855-1870.
- [5] Kerans C. Karst-controlled reservoir heterogeneity in Ellenberger Group carbonates of west Texas. *AAPG Bulletin*, 1988; 72: 1160-1183.
- [6] Wang BQ, and Ihsan S. Al-Aasm. Karst-controlled diagenesis and reservoir development: Example from the Ordovician main reservoir carbonate rocks on the eastern margin of the Ordos Basin, China. *AAPG Bulletin*, 2002; 86(9): 1639-1658.
- [7] Chung E, Ting KK, and Aljaaidi O. Karst modeling of a Miocene carbonate build-up in Central Luconia, SE Asia: Challenges in seismic characterisation and geological model building. *International Journal of Earth Sciences*, 2011; 14539.
- [8] Khazali NFM, Osman S, and Abdullah CS. The awakened giants. *Petroleum Geoscience Conference and Exhibition (PGCE)*, Kuala Lumpur, Malaysia, 2013; March 18-19.
- [9] Kosa E, Warrlich G, and Loftus G. Wings, Mushrooms, and Christmas trees: The carbonate seismic geomorphology of Central Luconia, Miocene – present, offshore Sarawak, northwest Borneo. *AAPG Bulletin*, 2015; 99(11): 2043-2075.
- [10] Mahmud OAB, and Saleh SB. Petroleum resources, Sarawak; Leong, KM., Ed.; The petroleum geology and resources of Malaysia, Kuala Lumpur: Petroliam Nasional Berhad (PETRONAS), 1999; 456-472.
- [11] Scherer FC. Exploration in East Malaysia over the past decade; Halbouty, MT. Ed.; Giant oil and gas fields of the decade 1968-1978, AAPG Memoir 30, 1980; 423-440.
- [12] Epting M. Sedimentology of carbonate platforms in Central Luconia, offshore Sarawak. *Bulletin of the Geological Society of Malaysia*, 1980; 12: 17-30.
- [13] Vahrenkamp VC, David F, Duijndam P, Newall M and Crevello P. Growth architecture, faulting, and karstification of a Middle Miocene carbonate platform, Luconia province, Offshore Sarawak, Malaysia; Eberli, GP, Masferro, JL, Sarg, JFR., Eds.; Seismic imaging of carbonate reservoirs and systems, AAPG Memoir 81, 2004; 329-350.
- [14] Dunham RJ. Classification of carbonate rocks according to depositional texture; Ham, WE., Ed.; Classification of Carbonate Rocks, AAPG Memoir, 1962; 1: 108-121.
- [15] Embry AF and Klovan JE. A Late Devonian reef tract on northeastern Banks Island, Northwest Territories. *Canadian Petroleum Geology*, 1971; 19: 720-781.
- [16] Choquette P and Pray L. Geologic Nomenclature and Classification of Porosity in Sedimentary Carbonates. *American Association of Petroleum Geologists Bulletin*, 1970; 54(2): 207-250.
- [17] Allan TL, Young MD, Peyaud J-B, Korsch MJ, and Whitford DJ. Strontium isotope stratigraphy of Miocene reservoir limestone from the Central Luconia Province, offshore Sarawak. *CSIRO Petroleum Confidential Report 08-025*, 2008.
- [18] Ali MY, and Abolins P. Central Luconia Province; Leong, KM., Ed.; The petroleum geology and resources of Malaysia, Kuala Lumpur: Petroliam Nasional Berhad (PETRONAS), 1999; 456-472.
- [19] Lunt P. Biogeography of some Eocene larger foraminifera, and their application in distinguishing geological plates. *Palaeontologia Electronica*, 2003; (6)1.
- [20] Wilson MEJ, and Vecsei A. The apparent paradox of abundant foramol facies in low latitudes: their environmental significance and effect on platform development. *Earth Science Reviews*, 2005; 69(1): 133-168.
- [21] Adams CG. The foraminifera and stratigraphy of the Melinau Limestone, Sarawak, and its importance in Tertiary correlation. *Quarterly Journal of the Geological Society of London*. 1965, 121: 283-238.
- [22] Lapre, Thornton. Carbonate stratigraphy of the SE Platform Complex, Central Luconia Province (unpublished). Shell report Exp. R.1741. 1970.
- [23] Lunt P. Foraminiferal micropalaeontology in SE Asia; Bowden, AJ, et al. Eds.; Landmarks in foraminiferal micropalaeontology: history and development, *The Micropalaeontological Society Spec. Publ. 6*, Geol. Soc. London, 2013; 193-206.

- [24] Coral Reef Alliance. Retrieved from <https://coral.org/coral-reefs-101/coral-reef-ecology>, 2018.
- [25] Roozpeykar A, and Moghaddam IM. Sequence biostratigraphy and paleoenvironmental reconstruction of the Oligocene-early Miocene deposits of the Zagros basin (Dehdasht area, South West Iran). *Arabian Journal of Geosciences*, 2016; 9:77.
- [26] Flugel E *Microfacies of carbonate rocks* (2nd edition). New York: Springer Heidelberg Dordrecht London, 2010.
- [27] Final Well Report (Drilling) Jintan-2. Occidental Petroleum (M) LTD, 1992. (unpublished)
- [28] Final Well Report, book 1 of 2, Jintan-3. OXY, 1997. (unpublished)
- [29] Yusliandi A. Influence of Local and Regional Factors Controlling the Evolution of the Miocene Mega Platform in the Central Luconia Province, Offshore Sarawak. Unpublished MSc. Thesis, Universiti Teknologi PETRONAS, 2020.
- [30] Martini E. Standard Tertiary and Quaternary calcareous nannoplankton zonation; Farinacci, A., Ed.; Proc. 2nd Int. Conf. Planktonic Microfossils Roma: Rome (ed. Tecnosci.). 1971; 2: 739–785.
- [31] Mohamed M. Biostratigraphic study of the Jintan-3 well, Sarawak Basin. Occidental Petroleum Malaysia LTD., 1997. (unpublished)
- [32] Haq BU, Hardenbol J, and Vail PR. Mesozoic and Cenozoic chronostratigraphy and cycles of sea-level change; *Sea-level changes: An integrated approach*, 1988; 71–108.
- [33] Lunt P. Tectono-stratigraphic development of the NW Borneo and South China Sea area. 2020. (Unpublished work)
- [34] Chung WK, Jamaludin FS and Ghosh D. Geomorphology and karstification of the Southern Field High Carbonates in Central Luconia. *Offshore Technology Conference*, 2016, March 1–3.
- [35] BouDagher-Fadel MK. *Evolution and Geological Significance of Larger Benthic Foraminifera*. Elsevier, Amsterdam, Netherlands, 2008.
- [36] Lunt P, and Madon M. A review of the Sarawak Cycles: history and modern application. *Bulletin of the Geological Society of Malaysia*, 2017; 63: 77-101.
- [37] Veenhof EN. A regional review of Balingian Province. Sarawak Shell Berhad exploration report 50800, 2 volumes, 1997. (unpublished).

---

*To whom correspondence should be addressed: Bing Bing Saw, South East Asia Clastic/Carbonate Research Laboratory, Institute of Hydrocarbon Recovery, Universiti Teknologi PETRONAS, Seri Iskandar, Perak 32610, Malaysia, E-mail: [bingbingsaw@gmail.com](mailto:bingbingsaw@gmail.com)*